GMR
The Original by FUNPEC-RP

Transcriptional profile of major genes related to X-chromosome inactivation during bovine embryonic development

L.N. Vargas[1,2], A.S.M. Soares[3], M.A.N. Dode[2,4,5], L.A.M.P. Melo[5] and M.M. Franco[1,2,5]

[1] Pós-Graduação em Genética e Bioquímica, Instituto de Biotecnologia, Universidade Federal de Uberlândia, Uberlândia, MG, Brasil
[2] Laboratório de Reprodução Animal, Embrapa Recursos Genéticos e Biotecnologia, Brasília, DF, Brasil
[3] Instituto Federal de Educação, Ciência e Tecnologia do Triângulo Mineiro, campus Uberaba Parque Tecnológico, Uberaba, MG, Brasil
[4] Pós-Graduação em Ciências Animais, Faculdade de Agronomia e Veterinária, Universidade de Brasília, Brasília, DF, Brasil
[5] Embrapa Recursos Genéticos e Biotecnologia, Brasília, DF, Brasil

Corresponding author: M.M. Franco
E-mail: mauricio.franco@embrapa.br

Genet. Mol. Res. 22 (4): gmr19144
Received March 06, 2023
Accepted September 13, 2023
Published October 09, 2023
DOI http://dx.doi.org/10.4238/gmr19144

ABSTRACT. X-chromosome inactivation (XCI), an essential epigenetic event in female embryos, is involved in embryonic development and requires refined control mechanisms. Although studies in cattle have been contributing to the understanding of the dynamic mechanisms of XCI, no research has yet investigated XCI in elongated bovine embryos. We used qPCR to characterize the mRNA levels of five target genes (*XIST*, *JPX*, *H2AFY*, *H2AFY2*, and *EZH2*) related to XCI in bovine embryos at stages: 8-16-cells (72 embryos), morula (72 embryos), blastocyst (64 embryos), hatched blastocyst (64 embryos), D11 blastocyst (20 embryos), and D14 (biopsies of 4 biopsies of embryos). Our results showed the same mRNA levels of *XIST*, *JPX*, and *H2AFY2* at the morula stage, which were higher than those of the other genes. However, *JPX* declined after the morula stage, whereas *XIST* and *H2AFY2* maintained higher mRNA levels in

BL and HB. The expression of *XIST* and *H2AFY2* reached the lowest levels at D11 and D14. We suggest that the changes in mRNA levels of these genes in the initial stages of development are related to the onset of XCI in cattle. This study is relevant to improve our understanding of the dynamic mechanisms that act in XCI in cattle until the elongated embryo stage.

Key words: X-chromosome inactivation; Gene Expression; Epigenetics; Embryogenesis

INTRODUCTION

In female mammals, one X chromosome is inactivated to obtain equivalent gene expression between females (XX) and males (XY) (Lyon 1961). X-chromosome inactivation (XCI) occurs during early embryonic development and is essential for supporting female embryo development (Borensztein et al. 2017). In short, the process is controlled by epigenetic factors and is well understood in mice (McCarrey and Dilworth 1992; Plath et al. 2002; Cerase et al. 2021; Markaki et al. 2021). Although XCI is relatively conserved in mammals, the inactivation mechanism does not follow a pattern among species (Dupont and Gribnau 2013).

In eutherians, XCI initiation is regulated by a control region, the X-inactivation center (XIC), where the X-inactive specific transcript (*XIST*) gene is located (Brown et al. 1991; Brockdorff et al. 1992). *XIST* is a major gene related to XCI initiation and is exclusively expressed on the inactive X chromosome (Finn et al. 2014). The activation of *XIST* expression involves a combination of events, such as expression of the long non-coding RNA (lncRNA) *JPX* (Tian et al. 2010). *JPX* is a positive regulator of *XIST* that induces its expression by preventing the binding of CTCF protein to the *XIST* promoter (Sun et al. 2013; Karner et al. 2020).

The future inactive X (Xi) chromosome expresses *XIST*, which coats the X chromosome and recruits chromatin remodelers polycomb repressive complex 1 (PRC1) and polycomb repressive complex 2 (PRC2). The catalytic subunit of PRC2, *EZH2*, modifies histone H3 lysine 27 trimethylation (H3K27me3) (de Napoles et al. 2004; Okamoto et al. 2004; Chaumeil et al. 2006). Subsequently, markers related to heterochromatin, such as the incorporation of the histone variant, MacroH2A, and DNA methylation, have been established to maintain and stabilize the inactive chromosome (Mermoud et al. 2002; Hernández-Muñoz et al. 2005; Jeon et al. 2012). These events are necessary for chromatin modification, changing the chromosome to a heterochromatic state and silencing the chromosome.

XCI is a major epigenetic event in female embryos (Loda et al. 2022). Consequently, the mechanisms related to XCI establishment are refined and must occur appropriately for embryo development (Tan et al. 2016). XCI may be affected by assisted reproductive techniques; therefore, understanding XCI-related events in livestock is essential. Studies in cattle have been contributing to the knowledge of the dynamic mechanisms of XCI (Chureau et al. 2002; Dindot et al. 2004; Ferreira et al. 2010; Mendonça et al. 2019; Yu et al. 2020; Castro et al. 2022); however, no studies have investigated XCI in elongated embryos.

This study aimed to characterize the mRNA levels of five major genes related to XCI in bovine embryos at stages 8-16-cells, morula, blastocyst (BL), hatched blastocyst (HB), D11 blastocyst, and D14 elongated embryos. The X-inactive specific transcript *XIST*, *Xist* activator lncRNA *JPX*, macroH2A.1 histone *H2AFY*, macroH2A.2 histone *H2AFY2*, and enhancer of zeste 2 polycomb repressive complex 2 subunit *EZH2* genes were analyzed.

MATERIAL AND METHODS

All experimental procedures involving animals were approved by the Animal Research Ethics Committee of the Biological Science Institute from Brasilia University Brazil, under license number UnBDOC 107942/2009.

In vitro embryo production

Embryos were produced as described by Mendonça et al. (2019) using female sex-sorted semen from a Gyr bull (ABS Pecplan, Brazil) with proven *in vitro* fertility and oocytes collected from bovine ovaries obtained in a local abattoir. The embryos were produced by *in vitro* fertilization and then collected at different stages, according to previous studies (Brandao et al. 2004; Ferreira et al. 2010; Mendonça et al. 2019; Leme et al. 2021): 8–16-cell (72 h post insemination), morula (144 h p.i.), blastocyst (156 h p.i.), hatched blastocyst (192 h p.i.), D11 (264 h p.i.), and D14 (336 h p.i.) (Figure 1). We collected four pools for all stages: 18 embryos/per pool of 8–16-cell, 18 embryos/per pool of morula, 16 blastocysts (BL)/per pool, 16 hatched blastocysts (HB)/per pool, five embryos on D11/per pool, and four biopsies of embryos on D14.

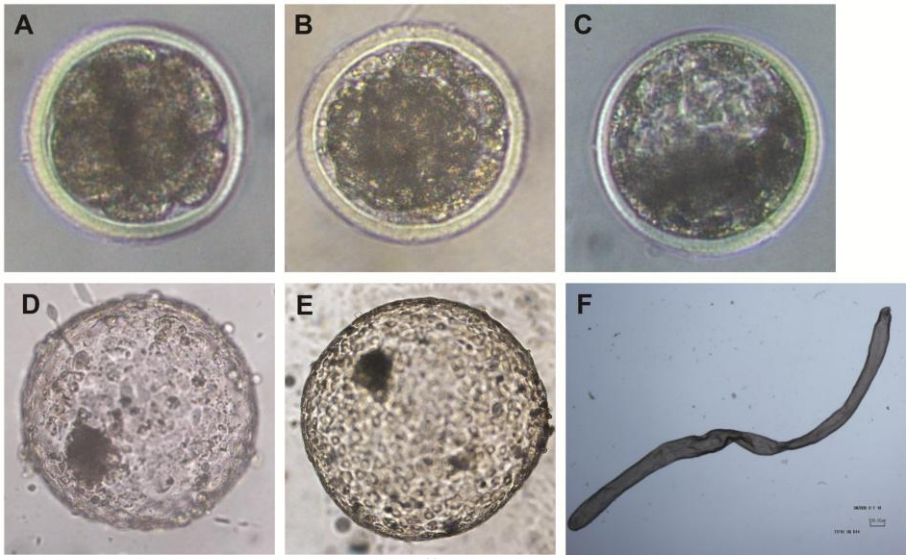

Figure 1. Bovine embryos produced *in vitro* in different stages. (A) 8–16-cell stage, (B) morula stage (C) blastocyst stage, (D) hatched blastocyst, (E) D11 blastocyst, and (F) D14.

RNA extraction, reverse transcription, and qPCR

Total RNA from pools of each embryo stage was isolated using the RNeasy Plus Micro Kit (Qiagen, Valencia, CA, USA). Carrier RNA was used during isolation according to the manufacturer's instructions. Total RNA samples were immediately subjected to cDNA synthesis using the GoScript™ Reverse Transcription System (Promega, Madison, WI, USA) with 0.5 µg random primer and 5 mM $MgCl_2$ in a final volume of 25 µL. After cDNA synthesis, the reaction volume was complete to 30 µL with nuclease-free water. The cDNA samples were stored at −20 °C until further use.

The relative mRNA abundance of genes related to XCI, *XIST*, *JPX*, *H2AFY*, *H2AFY2*, and *EZH2* was determined by RT-qPCR. Primers were designed using the PrimerQuest tool (http://www.idtdna.com/PrimerQuest) and are listed in Table 1. The RT-qPCR amplification mixtures were comprised of 1 µL cDNA, specific concentrations of each primer (Table 1), 12.5 µL of GoTaq qPCR Master Mix (Promega), and nuclease-free H_2O to a final volume of 25 µL. The reactions were performed with a 7500 Fast Real-Time PCR System (Applied Biosystems, Foster City, CA, USA). The cycling conditions included an initial step at 50 °C for 20 s and 95 °C for 10 min, followed by 40 cycles at 95 °C for 15 s (denaturation), and the annealing/extension temperature for 1 min (Table 1), with a melting curve at 65–95 °C. Primers with amplification efficiencies between 80-110% were used. Each sample was analyzed in triplicate, and PCR product specificity was determined by melting curve analysis and amplicon size in the agarose gel.

Table 1. Primers for RT-qPCR analysis of the genes XIST, JPX, H2AFY, H2AFY2, EZH2, GAPDH, and ACTB.

Gene	Primer sequence (5'-3')	Amplicon size (bp)	Primers concentration	Annealing temperature	Genbank accession number
XIST	F: GAAATGGGCCTAGTCTAAAGGG R: GGACCAGACTTCACCAAGAAA	159	200 nM	60 °C	XR_001495594.2
JPX	F: TGTAACGCAGGAGACACAAG R: GGGATTCTCCAGGCACAAATA	106	200 nM	60 °C	KU050194.1
H2AFY	F: GAAAGGCCACCCCAAGTACA R: CCCTGCCCTTCTTGTTGTCT	128	200 nM	60 °C	XM_005209376.2
H2AFY2	F: ACTGTCACATCCCTCAGTGG R: AATGCCACCGACTTCAGCTT	109	150 nM	61 °C	NM_001076086.1
EZH2	F: GGGCACAGCAGAAGAGCTAA R: AAGTGTTGGGTGTTGCATGA	230	500 nM	61 °C	NM_001193024.1 (Yu et al. 2020)
GAPDH	F: GGCGTGAACCACGAGAAGTATAA R: CCCTCCACGATGCCAAAGT	119	200 nM	60 °C	NM_001034034.2
ACTB	F: GGCACCCAGCACAATGAAGATCAA R: ATCGTACTCCTGCTTGCTGATCCA	134	200 nM	60 °C	NM_173979.3

Transcript levels were normalized to the amount of housekeeping genes encoding *Bos taurus* actin beta (*ACTB*) and *Bos taurus* glyceraldehyde-3-phosphate dehydrogenase (*GAPDH*). The geometric average of the cycle threshold (Ct) and of the efficiencies of the housekeeping genes were used for data normalization (Vandesompele et al. 2002). Considering that the zygotic genome activation in cattle occurs around 8-16 cells, the mean values of the 8–16-cell group were used as the reference sample. The relative abundance of each gene was calculated using the ΔΔCt method, with efficiency correction using the Pfaffl method (Pfaffl 2001).

Statistical analysis

Data were analyzed using GraphPad Prism (https://www.graphpad.com/scientific-software/prism/). Gene expression data were compared among multiple experimental groups using the Kruskal-Wallis test, followed by Dunn's multiple comparison test. Tukey's multiple comparison test was performed to compare the mean mRNA levels among different genes at each stage and to evaluate which mean mRNA levels among a set of means differed from the rest. P values ≤ 0.05 denote a statistically significant difference.

RESULTS

XIST mRNA levels showed no significant differences among the embryo stages (Figure 2A). In contrast, the transcript levels of *JPX* were downregulated from the 8–16-cell to HB stage (Figure 2B). We also investigated the expression of two histone variants macroH2A, *H2AFY* and *H2AFY2*. The *H2AFY* transcript levels decreased from the 8–16-cell stage to the HB and D11 stages; nevertheless, the mRNA level was relatively low and very stable from the morula stage to all subsequent stages of development analyzed (Figure 2C). In contrast, *H2AFY2* showed more variation among pools at each stage and during the development analyzed (Figure 2D). The mRNA levels of *H2AFY2* decreased significantly between the 8–16-cell and D14 stages (Figure 2D). *EZH2* exhibited a similar expression pattern to *H2AFY*, where lower mRNA levels were found after the 8–16-cell stage and were stable throughout embryonic development (Figure 2E). Significant differences were found in *EZH2* mRNA levels between 8–16-cell and the following stages: HB, D11, and D14 (Figure 2E).

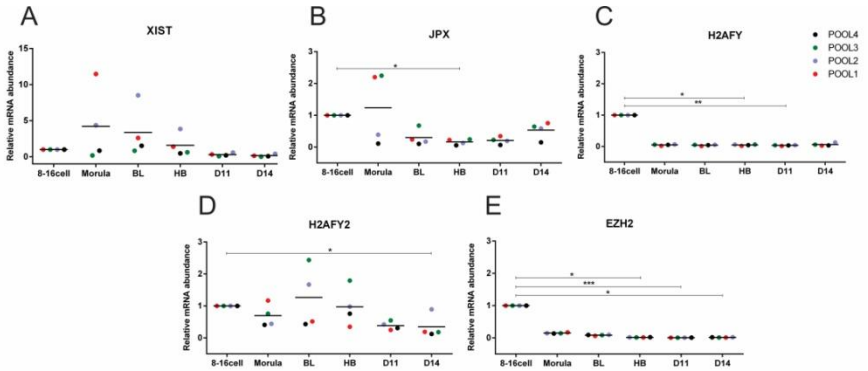

Figure 2. Relative abundance of mRNA of XCI-related genes *XIST*, *JPX*, *H2AFY*, *H2AFY2*, and *EZH2* determined by quantitative RT-qPCR. (A, B, C, D, E) Levels of mRNA from stages: 8–16-cell, morula, blastocyst (BL), hatched blastocyst (HB), D11, and D14 embryos in each gene. mRNA levels were analyzed in the four pools in all stages. (*) represents significantly different mean values using the Kruskal–Wallis test (P ≤ 0.05).

To determine whether the genes exhibited the same pattern of expression during the stages of development, we compared the mRNA levels between the genes in each stage. We identified similar mRNA levels of *XIST*, *JPX*, and *H2AFY2* in the morula stage (Figure 3). However, in the blastocyst stage, *JPX* expression decreased, whereas *XIST* and *H2AFY2* maintained higher mRNA levels until HB stage. Interestingly, mRNA levels of *XIST* and *H2AFY2* were similar during all embryonic developmental stages analyzed (Figure 3). In addition, *EZH2* and *H2AFY* expression decreased in the morula stage, from which the mRNA levels remained low and stable until D14.

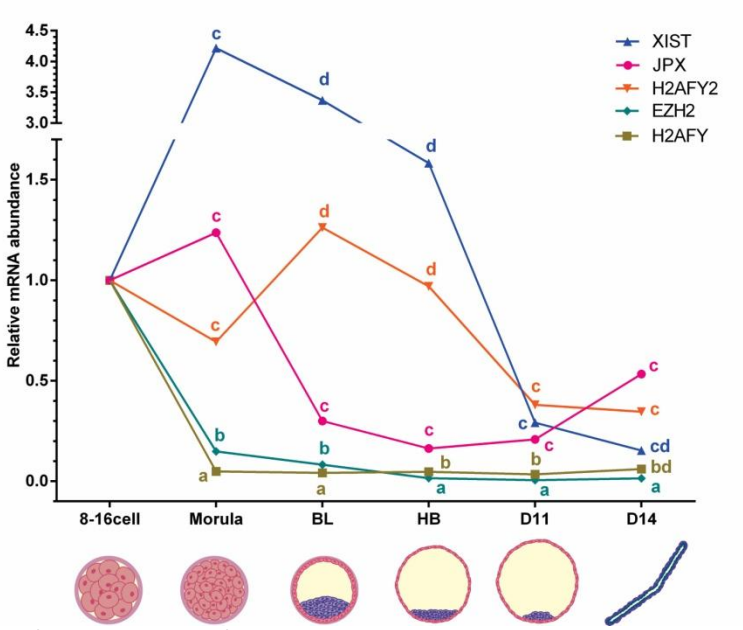

Figure 3. Profile of gene expression of the genes *XIST*, *JPX*, *H2AFY*, *H2AFY2*, and *EZH2* through bovine embryonic development. The stages analyzed were 8–16-cell, morula, blastocyst (BL), hatched blastocyst (HB), D11, and D14. The graph values represent the mean of four pools in each stage for all genes. Tukey's multiple comparison tests were used to determine differences in mRNA levels among the genes within the same embryonic stage. Different letters ($P < 0.05$) indicate significant differences among genes.

DISCUSSION

In eutherians, *XIST* is the central element for XCI initiation during early embryogenesis (Brockdorff et al. 1991; Brown et al. 1991). We found no significant differences in *XIST* expression; however, we observed more variability in mRNA levels between pools in the morula and blastocyst stages. Similarly, a previous study in cattle showed that *XIST* is upregulated in the morula stage (Yu et al. 2020). Moreover, *XIST* expression increased only in female embryos at the morula and blastocyst stages (Yu et al. 2020; Aksit et al. 2022). Interestingly, a study in cattle identified monoallelic expression of the monoamine oxidase A (*MAOA*), an X chromosome-linked gene, in the morula stage, indicating that the X chromosome is inactivated at this stage (Ferreira et al. 2010).

Here, we found high variation in the mRNA levels among samples in *XIST*, *JPX*, and *H2AFY2* genes during initial embryogenesis. Considering that XCI may initiate during

this window of development, we suppose this variation may indicate the diverse states of XCI between the cells of distinct samples. The lncRNA *JPX* is a positive regulator of *XIST*, and in mice, its expression is sufficient to activate *XIST* (Carmona et al. 2018). *JPX* triggers *XIST* expression by removing proteins from the *XIST* promoter (Sun et al. 2013). *JPX* expression is essential to XCI because its deletion blocks XCI and is lethal to female mouse embryos (Tian et al. 2010). Here, we found the same *JPX* and *XIST* levels at the morula stage, but *JPX* decreased to lower levels at the BL and HB stages. This result suggests that *JPX* decreases after contributing to an increase in *XIST* expression in the morula. A recent study in cattle reported that *JPX* expression decreased from zygote to the morula stage (Yu et al. 2020); however, the study did not analyze stages after blastocyst to the elongated embryo. Here, we showed that after blastocyst development, *XIST* expression decreased and reached the same *JPX* levels at D11 and D14. Therefore, if we consider the function of *JPX* triggering *XIST* expressions is conserved between mice and cows, our results may suggest *XIST* activation by *JPX* around the morula stage.

XCI maintenance requires the signatures of repressive chromatin, such as the incorporation of histone variant macroH2A, which typically co-localizes with H3K27me3 along Xi (Gamble et al. 2010). The heterochromatin mark H3K27me3 across the zygote genome is catalyzed by PRC2 (Meng et al. 2020). In cattle, the catalytic subunit of PRC2, *EZH2*, showed a peak in transcription at the 4-cell stage, after which it decreased in the 8-cell stage until BL (Duan et al. 2019). Another study showed stable *EZH2* expression until the 8-cell stage and declined until BL (Yu et al. 2020). We also found a decrease in *EZH2* mRNA levels after 8–16-cells, which remained low, constitutive, and very stable until the elongated embryo (D14).Another study in cattle showed nuclear expression of PRC2 members at the morula and blastocyst stages, which also correlated with increased H3K27me3 levels (Ross et al. 2008).

The histone macroH2A variants *H2AFY* and *H2AFY2* are known to be present in mouse and human Xi (Mermoud et al. 1999; Chadwick and Willard 2002). In cattle, immunofluorescence studies have indicated that *H2AFY* is preferentially localized on Xi, whereas *H2AFY2* does not appear to be associated with Xi (Coppola et al. 2008). Here, we observed the same expression pattern of *H2AFY2* and *XIST* through development and the low and constitutive *H2AFY* expression. Despite the preferential localization of macroH2As in Xi, XCI can occur in mouse embryonic stem cells with *H2AFY* and *H2AFY2* knockdown (Tanasijevic and Rasmussen 2011). However, in mice, *H2AFY* and *H2AFY2* knockout affects prenatal and postnatal growth and lipid metabolism (Boulard et al. 2010; Pehrson et al. 2014). Thus, macroH2A variant deficiency suggests that the heterochromatic state of Xi uses different epigenetic markers; however, *H2AFY* and *H2AFY2* play essential roles in other developmental biological functions (Douet et al. 2017; Hsu et al. 2021; Kumbhar et al. 2021).

In summary, we examined, for the first time, the players involved in XCI establishment in bovine until the elongated embryo. We found dynamic expression during the initial stages of the development of central elements for the initiation of XCI, *JPX* and *XIST*. After HB, these genes showed lower and regular expression until D14. We suggest that the dynamic mRNA levels of these genes in the initial stages of development are related to the onset of XCI in cattle. Finally, our results are relevant to improve our understanding of the dynamic mechanisms that act in XCI in cattle.

ACKNOWLEDGMENTS

We thank CNPq, Brazil, and Embrapa Genetic Resources and Biotechnology, Brazil, for providing support for this study.

AUTHOR CONTRIBUTIONS

A.S.M. conducted sample collection. L. N. V. and L.A.M.P. performed the statistical analyses. L.N.V and M.M.F. performed genomic analyses. L.N.V., M.A.N.D. and M.M.F. designed the experiments. L.N.V. and M.M.F interpreted the results and wrote the manuscript. All authors have read and approved the final manuscript.

CONFLICTS OF INTEREST

The authors declare no conflict of interest.

REFERENCES

Aksit MA, Yu B, Roelen BAJ and Migeon BR (2022). Silencing XIST on the future active X: Searching human and bovine preimplantation embryos for the repressor. *Eur. J. Hum. Genet.* 19: 1-8.

Borensztein M, Syx L, Ancelin K, Diabangouaya P, et al. (2017). Xist-dependent imprinted X inactivation and the early developmental consequences of its failure. *Nat. Struct. Mol. Biol.* 24: 226-33.

Boulard M, Storck S, Cong R, Pinto R, et al. (2010). Histone variant macroH2A1 deletion in mice causes female-specific steatosis. *Epigenetics Chromatin.* 3: 8.

Brandao DO, Maddox-Hyttel P, Lovendahl P, Rumpf R, et al. (2004). Post hatching development: a novel system for extended in vitro culture of bovine embryos. *Biol. Reprod.* 71: 2048-55.

Brockdorff N, Ashworth A, Kay GF, Cooper P, et al. (1991). Conservation of position and exclusive expression of mouse Xist from the inactive X chromosome. *Nature.* 351: 329-31.

Brockdorff N, Ashworth A, Kay GF, McCabe VM, et al. (1992). The Product of the Mouse Xist Gene Is a 15 kb Inactive X-Specific Transcript Containing No Consewed ORF and Located in the Nucleus. *Cell.* 71: 515-26.

Brown CJ, Lafreniere RG, Powers VE, Sebastio G, et al. (1991). Localization of the X inactivation centre on the human X chromosome in Xq13. *Nature.* 349: 82-4.

Carmona S, Lin B, Chou T, Arroyo K, et al. (2018). LncRNA Jpx induces Xist expression in mice using both trans and cis mechanisms. *PLoS Genet.* 14: e1007378.

Castro PS, Vargas LN, Silva TCF, Rios AFL, et al. (2022). Research Article Transcriptional profile throughout the X-inactive specific transcript (XIST) locus in the placenta of cattle. *Genet. Mol. Res.* 21(2): GMR19039.

Cerase A, Young AN, Ruiz NB, Buness A, et al. (2021). Chd8 regulates X chromosome inactivation in mouse through fine-tuning control of Xist expression. *Commun. Biol.* 4: 485.

Chadwick BP and Willard HF (2002). Cell cycle-dependent localization of macroH2A in chromatin of the inactive X chromosome. *J. Cell Biol.* 157: 1113-23.

Chaumeil J, Le Baccon P, Wutz A and Heard E (2006). A novel role for Xist RNA in the formation of a repressive nuclear compartment into which genes are recruited when silenced. *Genes Dev.* 20: 2223-37.

Chureau C, Prissette M, Bourdet A, Barbe V, et al. (2002). Comparative sequence analysis of the X-inactivation center region in mouse, human, and bovine. *Genome Res.* 12: 894-908.

Coppola G, Pinton A, Joudrey EM, Basrur PK, et al. (2008). Spatial distribution of histone isoforms on the bovine active and inactive X chromosomes. *Sex Dev* 2, 12-23.

de Napoles M, Mermoud JE, Wakao R, Tang YA, et al. (2004). Polycomb group proteins Ring1A/B link ubiquitylation of histone H2A to heritable gene silencing and X inactivation. *Dev. Cell.* 7: 663-76.

Dindot SV, Kent KC, Evers B, Loskutoff N, et al. (2004). Conservation of genomic imprinting at the XIST, IGF2, and GTL2 loci in the bovine. *Mamm Genome.* 15: 966-74.

Douet J, Corujo D, Renauld RMJ, Sansoni V, et al. (2017). MacroH2A histone variants maintain nuclear organization and heterochromatin architecture. *J. Cell Sci.* 130: 1570-82.

Duan J, Zhu L, Dong H, Zheng X, et al. (2019). Analysis of mRNA abundance for histone variants, histone- and DNA-modifiers in bovine in vivo and in vitro oocytes and embryos. *Sci. Rep.* 9: 1217.

Dupont C and Gribnau J (2013). Different flavors of X-chromosome inactivation in mammals. *Cell Biol.* 25: 314-21.

Ferreira AR, Machado GM, Diesel TO, Carvalho JO, et al. (2010). Allele-specific expression of the MAOA gene and X chromosome inactivation in in vitro produced bovine embryos. *Mol. Reprod. Dev.* 77: 615-21.

Finn EH, Smith CL, Rodriguez J, Sidow A, et al. (2014). Maternal bias and escape from X chromosome imprinting in the midgestation mouse placenta. *Dev. Biol.* 390: 80-92.

Gamble MJ, Frizzell KM, Yang C, Krishnakumar R, et al. (2010). The histone variant macroH2A1 marks repressed autosomal chromatin, but protects a subset of its target genes from silencing. *Genes Dev.* 24: 21-32.

Hernández-Muñoz I, Lund AH, Van Der Stoop P, Boutsma E, et al. (2005). Stable X chromosome inactivation involves the PRC1 Polycomb complex and requires histone MACROH2A1 and the CULLIN3/SPOP ubiquitin E3 ligase. *Proc. Natl. Acad. Sci. USA.* 102: 7635-40.

Hsu CJ, Meers O, Buschbeck M and Heidel FH (2021). The Role of MacroH2A Histone Variants in Cancer. *Cancers (Basel).* 13: 3003.

Jeon Y, Sarma K and Lee JT (2012). New and Xisting regulatory mechanisms of X chromosome inactivation. *Curr Opin Genet. Dev.* 22: 62-71.

Karner H, Webb CH, Carmona S, Liu Y, et al. (2020). Functional Conservation of LncRNA JPX Despite Sequence and Structural Divergence. *J. Mol. Biol.* 432(2): 283-300.

Kumbhar R, Sanchez A, Perren J, Gong F, et al. (2021). Poly(ADP-ribose) binding and macroH2A mediate recruitment and functions of KDM5A at DNA lesions. *J. Cell Biol.* 220: e202006149.

Leme LO, Machado GM, Fidelis AAG, Guimaraes ALS, et al. (2021). Transcriptome of D14 in vivo x in vitro bovine embryos: is there any difference? *In Vitro Cell Dev. Biol. Anim.* 57(6): 598-609.

Loda A, Collombet S and Heard E (2022). Gene regulation in time and space during X-chromosome inactivation. *Nat. Rev. Mol. Cell Biol.* 23(4): 231-49.

Lyon MF (1961). Gene action in the X-chromosome of the mouse. *Nat. Genet.* 190(4773): 372-3.

Markaki Y, Gan Chong J, Wang Y, Jacobson EC, et al. (2021). Xist nucleates local protein gradients to propagate silencing across the X chromosome. *Cell.* 184: 6174-92 e32.

McCarrey JR and Dilworth DD (1992). Expression of Xist in mouse germ cells correlates with X-chromosome inactivation. *Nat. Genet.* 2: 200-3.

Mendonça ADS, Silveira MM, Rios ÁFL, Mangiavacchi PM, et al. (2019). DNA methylation and functional characterization of the XIST gene during in vitro early embryo development in cattle. *Epigenetics.* 14: 568-88.

Meng TG, Zhou Q, Ma XS, Liu XY, et al. (2020). PRC2 and EHMT1 regulate H3K27me2 and H3K27me3 establishment across the zygote genome. *Nat. Commun.* 11: 6354.

Mermoud JE, Costanzi C, Pehrson JR and Brockdorff N (1999). Histone MacroH2A1.2 Relocates to the Inactive X Chromosome after Initiation and Propagation of X-Inactivation. *J. Cell Biol.* 147: 1399-408.

Mermoud JE, Popova B, Peters AH, Jenuwein T, et al. (2002). Histone H3 lysine 9 methylation occurs rapidly at the onset of random X chromosome inactivation. *Curr. Biol.* 12: 247-51.

Okamoto I, Otte AP, Allis CD, Reinberg D, et al. (2004). Epigenetic dynamics of imprinted X inactivation during early mouse development. *Science.* 303(5658): 644-9.

Pehrson JR, Changolkar LN, Costanzi C and Leu NA (2014). Mice without macroH2A histone variants. *Mol. Cell Biol.* 34: 4523-33.

Pfaffl MW (2001). A new mathematical model for relative quantification in real-time RT-PCR. *Nucleic Acids Res.* 29: e45.

Plath K, Mlynarczyk-Evans S, Nusinow DA and Panning B (2002). Xist RNA and the mechanism of X chromosome inactivation. *Annu Rev. Genet.* 36: 233-78.

Ross PJ, Ragina NP, Rodriguez RM, Iager AE, et al. (2008). Polycomb gene expression and histone H3 lysine 27 trimethylation changes during bovine preimplantation development. *Reproduction.* 136: 777-85.

Sun S, Del Rosario BC, Szanto A, Ogawa Y, et al. (2013). Jpx RNA activates Xist by evicting CTCF. *Cell* 153, 1537-51.

Tan K, An L, Miao K, Ren L, et al. (2016). Impaired imprinted X chromosome inactivation is responsible for the skewed sex ratio following in vitro fertilization. *Proc. Natl. Acad. Sci. USA.* 113: 3197-202.

Tanasijevic B and Rasmussen TP (2011). X chromosome inactivation and differentiation occur readily in ES cells doubly-deficient for macroH2A1 and macroH2A2. *PLoS One.* 6: e21512.

Tian D, Sun S and Lee JT (2010). The long noncoding RNA, Jpx, is a molecular switch for X chromosome inactivation. *Cell.* 143: 390-403.

Vandesompele J, De Preter K, Pattyn F, Poppe B, et al. (2002). Accurate normalization of real-time quantitative RT-PCR data by geometric averaging of multiple internal control genes. *Genome Biol.* 3: 1-12.

Yu B, van Tol HTA, Stout TAE and Roelen BAJ (2020). Initiation of X Chromosome Inactivation during Bovine Embryo Development. *Cells.* 9: 1016.